

**Localized electron states and spin polarization in Co/Ni(111) overlayers**

F. Gimbert and L. Calmels

*CEMES-CNRS, Université de Toulouse, 29 rue Jeanne Marvig, BP 94347, F-31055 Toulouse Cedex 4, France*

S. Andrieu

*Institut Jean Lamour, Nancy Université/CNRS, BP 239, F-54506 Vandoeuvre-lès-Nancy, France*

(Received 4 April 2011; revised manuscript received 1 July 2011; published 21 September 2011)

We used a surface-dedicated first-principles method to calculate the electronic structure in Co/Ni(111) overlayers with a Co thickness varying between 1 and 5 monolayers. We describe the majority and minority spin surface states, resonances, and quantum-well states and their dispersion, the energy and the number of these states depending on the Co-layer thickness. The difference between the total density of states and spin polarization of the different overlayers is found to be more important above the Fermi level. These results could be useful to analyze the surface-state spectra (spin-resolved direct and inverse photoemission, scanning tunneling spectroscopy) recorded *in situ* during the growth of Ni/Co multilayers for spintronic and nanomagnetism applications.

DOI: [10.1103/PhysRevB.84.094432](https://doi.org/10.1103/PhysRevB.84.094432)

PACS number(s): 73.20.At, 73.21.Fg, 75.70.Cn, 75.70.Rf

**I. INTRODUCTION**

The advances made during the last decades in the fields of ultrahigh-vacuum techniques and crystal growth have allowed the production of new epitaxial nanostructures, with unexpected physical properties due to the symmetry breaking of the electron states at the surfaces or at the interfaces. More precisely, the modification of the electronic and magnetic properties in multilayers can be explained in terms of the localized electron states with specific spin orientation and symmetry, which appear in the vicinity of the interfaces, or in terms of the interface-induced degeneracy lifting between states which would have the same energy in bulk materials. This has important consequences on the magnetic moments, the magnetic anisotropy, and the spin polarization, which can be analyzed using spectroscopic methods, magnetometry, or first-principles calculations. Several *in situ* spectroscopic techniques used to measure electron states during the growth of ultrathin layers being surface sensitive,<sup>1,2</sup> the calculations which are performed to analyze these experiments must not neglect the presence of the surface.

Co/Ni(111) superlattices with perpendicular magnetic anisotropy have in particular recently attracted attention because of their potential applications in magnetic memories switched by a relatively small spin transfer torque.<sup>3,4</sup> For this reason, studying the electron states in Co/Ni(111) multilayers by spectroscopic methods and first-principles calculations represents a challenge. Co/Ni systems have been investigated by several techniques in the recent years. The clean Ni(111) surface has first been studied by direct<sup>5-8</sup> and inverse<sup>9</sup> photoemission spectroscopy and by scanning tunneling spectroscopy (STS),<sup>10</sup> and surface states have been measured in an energy range between  $-0.25$  and  $0.1$  eV at the center of the surface Brillouin zone ( $\bar{\Gamma}$ ). The local density of states (DOS) has been calculated for this surface using a Ni slab, but DOS peaks related to surface states are not easy to identify because the slab used for this calculation is rather thin.<sup>11</sup> More sophisticated methods have further been used to study the surface-state energy dispersions of Ni(111).<sup>12</sup> The spin magnetic moment is generally found higher at the Ni(111) surface or in the subsurface layer than in bulk Ni.<sup>11,13,14</sup> The hexagonal compact

(hcp) Co(0001) surface has been studied by direct<sup>8,15-17</sup> and inverse<sup>18</sup> photoemission, and by STS.<sup>19</sup> Surface states have been observed between  $-0.43$  and  $0.9$  eV. Calculations have shown that a surface state exists near  $-0.5$  eV.<sup>19,20</sup> An enhancement of the spin magnetic moment has also been calculated for this surface.<sup>14,21</sup> The face centered cubic (fcc) Co(111) surface has only been studied theoretically<sup>14,20</sup> and shows a similar behavior to the hcp Co(0001) surface. Electron states in Co/Ni(111) superlattices have been investigated by first-principles calculations, but available results describe the total DOS and not the Bloch vector-resolved DOS.<sup>22</sup> Co overlayers deposited on a Ni substrate have been studied by inverse photoemission for a (001) but not for a (111) stacking.<sup>23</sup> An interface state has been reported for this system, but quantum-well (QW) states localized in the Co overlayers have not been observed. Magnetic moments have also been measured and calculated for Ni-terminated Ni/Co overlayers.<sup>24-26</sup>

In this paper, we describe the local DOS calculated near the surface of Co/Ni(111) overlayers with a Co thickness varying between 1 monolayer (ML) and 5 MLs. We investigated the different electron states which can exist in such nanostructures—QW states, surface states, and surface resonances—and we study their dispersion and orbital character. We also describe the surface spin polarization and spin magnetic moments. The DOS curves which we represent can be used to analyze photoemission and scanning tunneling spectra. Beyond the interpretation of electron spectra, our results could also be useful to understand the physical properties of Co/Ni(111) superlattices.

**II. QUANTUM-WELL, RESONANCE, AND SURFACE STATES IN Co/Ni(111) OVERLAYERS AT  $\bar{\Gamma}$** 

We calculated the electronic structure of Co( $n$ MLs)/Ni(111) overlayers with the multiple scattering code Layer Korringa Kohn Rostoker (layer-KKR)<sup>27,28</sup> which is based on the density functional theory (DFT) and uses the local spin density approximation (LSDA). This code is particularly well adapted for studying nanostructures which

only possess a two-dimensional periodicity such as surfaces and interfaces, the presence of a semi-infinite substrate being explicitly taken into account in the calculation. The lattice parameter which has been used for the overlayers is that of the bulk nickel substrate (0.352 nm) and we neglected atomic-layer relaxation or reconstruction in the vicinity of the surface. This is justified because the lattice parameter of fcc Ni is very close to that of fcc Co and to the interatomic distance in the (0001) atomic layers of hcp cobalt. We studied overlayers with a fcc stacking, which is reasonable for Co thicknesses up to 5 MLs,<sup>29</sup> using an atomic-sphere radius of 0.137 nm for all the atoms, a maximum angular momentum  $l_{\max} = 3$ , and a mesh of 45 Bloch vectors to perform integrations over the irreducible wedge of the two-dimensional first Brillouin zone. We used 5 layers of empty spheres on the vacuum side and 8 monolayers of nickel atoms between the Ni substrate and the Co overlayer, in which the electron density is free to change during the successive iterations of the self-consistent calculation, the Fermi level being that of bulk nickel.

The electron Bloch states which can exist in the vicinity of the (111) overlayers are the Ni substrate bulklike states, the Ni/Co interface states, the Co QW states, and the surface states. All these states depend on the two-dimensional Bloch vector  $\mathbf{k}_{\parallel}$ , and in the following we will first describe states at  $\bar{\Gamma}$  ( $\mathbf{k}_{\parallel} = \mathbf{0}$ ,  $\Gamma\bar{L}$  direction of the Ni substrate). The orbital character of these states will be discussed using  $x$ ,  $y$ , and  $z$  axes respectively parallel to the  $[\bar{1}10]$ ,  $[\bar{1}\bar{1}2]$ , and  $[111]$  directions of the Ni substrate. The point group of the  $\bar{\Gamma}$  point being  $C_{3v}$ , both for the fcc substrate<sup>30</sup> and for the (111) surface,<sup>31,32</sup> electron states at the center of the two-dimensional Brillouin zone will only have the  $A_1$  (linear combination of  $s$ ,  $p_z$ , and  $d_{z^2}$  atomic orbitals) or the  $E$  ( $p_x$ ,  $p_y$ ,  $d_{xz}$ ,  $d_{yz}$ ,  $d_{xy}$ , and  $d_{x^2-y^2}$ ) symmetry.<sup>30</sup> Along the  $\Gamma\bar{L}$  direction, the bulk Ni band structure consists in 4 valence bands for each spin direction,<sup>33,34</sup> with the  $A_1$  symmetry for the two lowest bands and the  $E$  symmetry for the other two flat bands. The band structure of fcc Ni and fcc Co is represented in Fig. 1.

Localized surface states with the  $A_1$  or the  $E$  symmetry can only be found in the energy gaps of the Ni substrate of the same symmetry. At the  $\bar{\Gamma}$  point and for the  $A_1$  symmetry, these energy gaps are found: below  $-9.17$  eV, between  $-4.8$  and  $-2.7$  eV, and above  $-0.58$  eV for majority spin, and below  $-9.13$  eV, between  $-4.39$  and  $-2.14$  eV, and above  $-0.56$  eV for minority spin. At  $\bar{\Gamma}$  and for the  $E$  symmetry, the Ni band gaps are found: below  $-2.41$  eV, between  $-2.14$  and  $-1.36$  eV, and above  $-0.58$  eV for majority spin, and below  $-1.78$  eV, between  $-1.48$  and  $-0.67$  eV, and above  $0.16$  eV for minority spin.

Co quantum-well states can also be found in the Ni band gaps, but at energies where bulk Co bands exist. At the  $\bar{\Gamma}$  point and for the  $A_1$  symmetry, the energy intervals where Co QW states can be found are as follows: between  $-3$  and  $-2.7$  eV for majority spin and between  $-4.39$  eV and  $-4.14$  eV for minority spin; at  $\bar{\Gamma}$  and for the  $E$  symmetry, Co QW states can be found between  $-2.6$  and  $-2.41$  eV and between  $-1.5$  and  $-1.36$  eV for majority spin and between  $-1.13$  and  $-0.78$  eV and between  $0.19$  and  $1.18$  eV for minority spin.

Figure 2 shows the majority spin (dark curves) and minority spin (red curves) local DOS with  $A_1$  symmetry integrated over

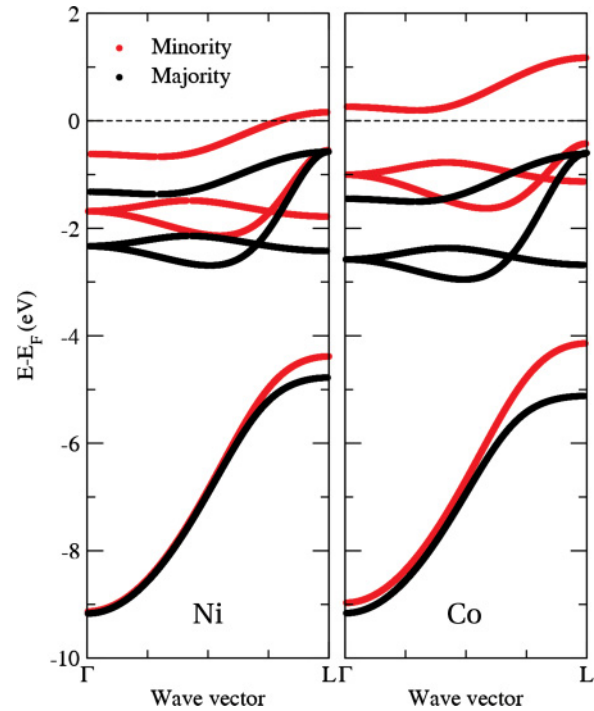


FIG. 1. (Color online) Band structure of bulk fcc Ni (left side) and fcc Co (right side) for wave vector along  $\Gamma\bar{L}$  ( $\mathbf{k}_{\parallel} = \mathbf{0}$  and  $k_z \neq 0$ ). Majority and minority spin bands are respectively shown with dark and red lines.

a Co atomic sphere of the surface layer, as a function of the Co overlayer thickness. Several peaks, which correspond to localized states, can be observed in the energy gaps of the substrate. The energy ranges where Co QW states are expected are indicated by gray (majority spin) and red (minority spin) shaded areas. For each of the Co( $n$ MLs)/Ni overlayers, we have compared the results presented in Fig. 2 with those calculated for Ni/Co( $n$ MLs)/Ni stacking<sup>35</sup> to determine whether the localized states are surface or quantum-well states (surface states do not exist in the case of a buried cobalt quantum well). We found a majority spin unoccupied surface state near  $0.43$  eV, independently of the overlayer thickness. The corresponding minority spin surface state has an energy of  $0.7$  eV for Co(1ML)/Ni; this state is shifted by  $0.07$  eV toward higher energy when the Co overlayer is thicker than 1 ML. Table I describes the charge density distribution of this minority spin surface state. It is mostly located in the surface Co atomic layer and in the first empty sphere layer, independently of the Co layer thickness, which explains that the surface state energy is not very sensitive to the nature of the subsurface atoms. Similar conclusions are obtained for the majority spin surface state. The number and the energy of the QW states depend on the number of cobalt MLs. The lowest energy majority spin QW state shifts from  $-2.75$  eV for Co(1ML)/Ni to  $-2.88$  eV for Co(5MLs)/Ni. A second QW state appears from 4 Co MLs; this state is stuck to the former one for a cobalt thickness of 5 MLs. For thicker overlayers, all the QW states gather in an energy range between  $-3$  and  $-2.7$  eV where the DOS is high for bulk fcc Co and for the corresponding (111) Co surface. A minority spin occupied quantum-well state can be observed near  $-4.3$  eV when the

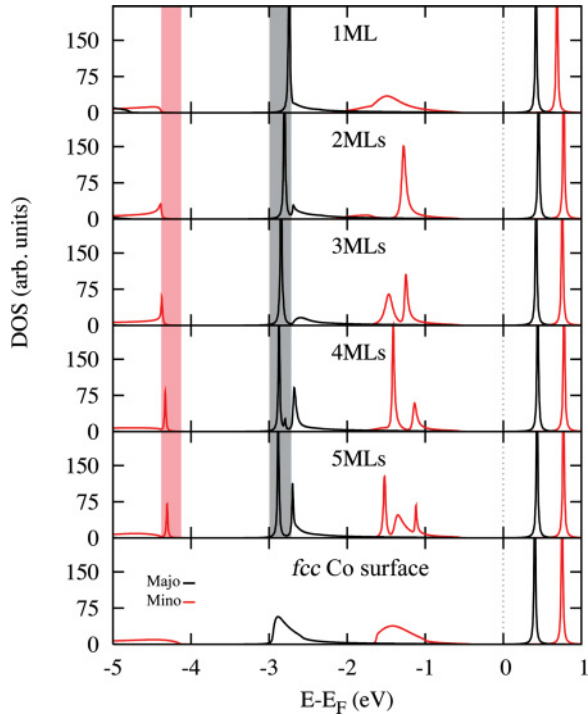


FIG. 2. (Color online) Majority spin (dark lines) and minority spin (red lines) partial DOS with  $A_1$  symmetry and  $\mathbf{k}_{\parallel} = \mathbf{0}$ , for a surface Co atom of the  $\text{Co}(n\text{MLs})/\text{Ni}(111)$  overlayers. From the top to the bottom, the different panels correspond to overlayers with  $n = 1$  to 5, and to the (111) fcc Co surface. The gray and red shaded areas respectively correspond to the energy ranges where majority and minority spin Co QW states can exist.

overlayer thickness is greater than 3 MLs. Peaks are also observed for minority spin between  $-1.55$  and  $-1.10$  eV. They correspond to resonance states and not to genuine QW states, because they are located inside an energy band of nickel with the same symmetry. The number of resonance states increases with the Co thickness from 1 state for  $\text{Co}(1\text{ML})/\text{Ni}$  and  $\text{Co}(2\text{MLs})/\text{Ni}$ , to 2 states for  $\text{Co}(3\text{MLs})/\text{Ni}$  and  $\text{Co}(4\text{MLs})/\text{Ni}$ , and 3 states for  $\text{Co}(5\text{MLs})/\text{Ni}$ . When the overlayer becomes thicker, the energy of the resonance states gathers between  $-1.63$  and  $-1.01$  eV, the energy range where the ( $s + p_z + d_z$ ) DOS is high in bulk fcc Co and at the  $\text{Co}(111)$  surface; see Fig. 2.

Figure 3 shows the majority and minority spin local DOS with  $E$  symmetry for a surface Co atom of the  $\text{Co}(n\text{MLs})/\text{Ni}$

TABLE I. Charge density distribution of the minority spin unoccupied surface state with an energy of 0.75 eV at  $\bar{\Gamma}$ , for the overlayers  $\text{Co}(1\text{ML})/\text{Ni}$ ,  $\text{Co}(2\text{MLs})/\text{Ni}$ , and  $\text{Co}(3\text{MLs})/\text{Ni}$ . The arbitrary unit numbers in this table correspond to the height of the surface state peak for a Co atom of the surface layer (S), for atoms of the successive sublayers (S - 1, S - 2, and S - 3), and for the empty sphere layers above the surface (S + 1 and S + 2).

	S - 3	S - 2	S - 1	S	S + 1	S + 2
Co(1ML)/Ni	4	10	28	100	72	2
Co(2MLs)/Ni	3	9	30	100	72	2
Co(3MLs)/Ni	3	10	31	100	74	2

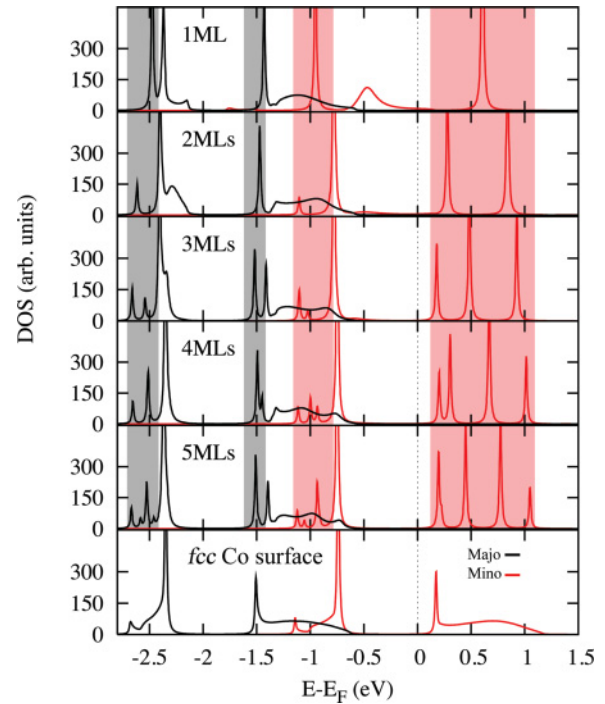


FIG. 3. (Color online) Same as in Fig. 2, but for localized states with  $E$  symmetry.

stacking, as a function of the Co-layer thickness. The comparison with DOS curves calculated for buried quantum wells<sup>35</sup> shows that the minority spin intense peak near  $-0.75$  eV, which appears from a thickness of 2 MLs, is a surface state [a similar conclusion could be drawn by comparison with the DOS calculated for the (111) fcc Co surface]. DOS peaks can be observed in the energy ranges where QW states are expected (shaded areas in the figure). For minority spin, the number of quantum-well states increases with the Co thickness. These QW states are shifted toward lower energies below  $-0.67$  eV and toward higher energies above 0.16 eV, when the Co thickness increases. They respectively have a strong ( $d_{xy} + d_{x^2-y^2}$ ) and ( $d_{xz} + d_{yz}$ ) character. The majority spin intense peak at  $-2.37$  eV is a resonance state because it is located in a continuum of the nickel substrate; it would correspond to a surface state for the pure fcc  $\text{Co}(111)$  surface.

### III. DISPERSION OF THE LOCALIZED ELECTRON STATES ALONG THE $\bar{\Gamma}\bar{M}$ AND $\bar{\Gamma}\bar{K}$ DIRECTIONS

We have calculated the dispersion of the surface and QW states in the high-symmetry directions of the two-dimensional Brillouin zone. The results obtained for  $\text{Co}(1\text{ML})/\text{Ni}(111)$  and for  $\mathbf{k}_{\parallel}$  along  $\bar{\Gamma}\bar{M}$  ( $[\bar{1}\bar{1}2]$  direction) are shown in Fig. 4. The curves represented in this figure describe the energy of the localized electron states as a function of the wave vector  $\mathbf{k}_{\parallel}$ , until these states cross a continuum of bulklike states. The localized states which have the strongest parabolic dispersion toward higher energies are the unoccupied surface states (SS). The dispersion is lower for the QW states, which split along  $\bar{\Gamma}\bar{M}$  except when the energy range available for these states is too small. We found nearly the same energies for the dispersion along  $\bar{\Gamma}\bar{K}$  ( $[\bar{1}10]$  direction); small differences between the

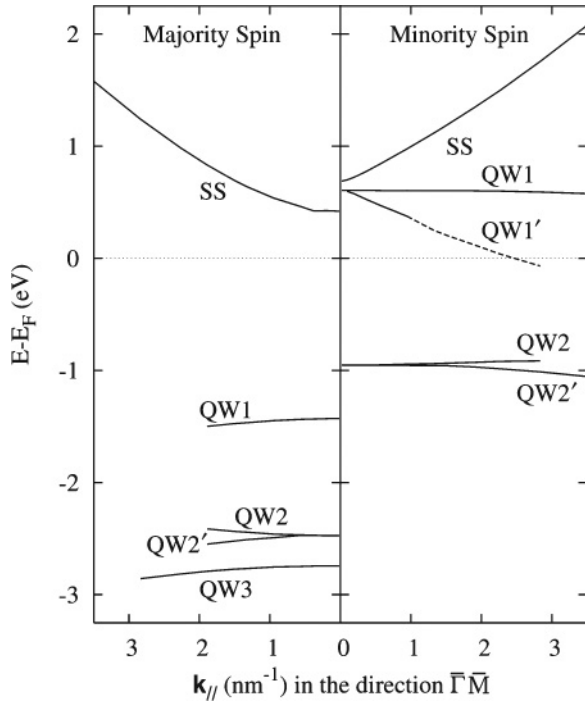


FIG. 4. Dispersion of the majority spin (left side) and minority spin (right side) surface states (SS) and quantum-well states (QW1, QW1', QW2, QW2', and QW3) along the  $\bar{\Gamma}\bar{M}$  direction, for the Co(1ML)/Ni(111) overlayer. The ends of the lines correspond to the point where localized states cross a bulk state continuum and vanish; for the minority spin quantum-well state QW1', an intense DOS peak persists when the state crosses the bulk continuum (dashed line in the figure).

dispersion along  $\bar{\Gamma}\bar{K}$  and  $\bar{\Gamma}\bar{M}$  only appear for wave vectors greater than  $3 \text{ nm}^{-1}$ .

The orbital character of the localized states represented in Fig. 4 can be understood from a group theory analysis. The point group of  $\mathbf{k}_{\parallel}$  along the  $\bar{\Sigma}$  ( $\bar{\Gamma}\bar{M}$ ) direction is  $C_s$  with the  $yz$ -mirror plane, and the corresponding irreducible representations are  $A'$  (linear combination of  $s$ ,  $p_y$ ,  $p_z$ ,  $d_{z^2}$ ,  $d_{yz}$ ,  $d_{x^2-y^2}$  atomic orbitals) and  $A''$  ( $p_x$ ,  $d_{xz}$ ,  $d_{xy}$ ).<sup>30</sup> Identity being the only symmetry operation for  $\mathbf{k}_{\parallel}$  along the  $\bar{T}$  ( $\bar{\Gamma}\bar{K}$ ) direction, all the electron states in this case belong to the  $A$

TABLE II. Symmetry and main orbital character of the majority and minority spin surface and QW states for  $\mathbf{k}_{\parallel}$  along  $\bar{\Gamma}\bar{M}$ . The labeling of the states is the same as in Fig. 4.

Name	Spin	Symmetry	Main Contributions
SS	Minority	$A'$	$p_z, d_{yz}$
SS	Majority	$A'$	$p_z$
QW1	Minority	$A''$	$d_{xz}$
QW1'	Minority	$A'$	$d_{yz}$
QW1	Majority	$A' + A''$	$d_{xz}, d_{yz}$
QW2	Minority	$A''$	$d_{xy}$
QW2'	Minority	$A'$	$d_{x^2-y^2}$
QW2	Majority	$A''$	$d_{xy}$
QW2'	Majority	$A'$	$d_{x^2-y^2}$
QW3	Majority	$A'$	$d_{z^2}, d_{yz}$

TABLE III. Same as in Table II, but for  $\mathbf{k}_{\parallel}$  along  $\bar{\Gamma}\bar{K}$ .

Name	Spin	Symmetry	Main Contributions
SS	Minority	$A$	$p_z, d_{xz}$
SS	Majority	$A$	$p_z$
QW1	Minority	$A$	$d_{yz}$
QW1'	Minority	$A$	$d_{xz}$
QW1	Majority	$A$	$d_{xz}, d_{yz}$
QW2	Minority	$A$	$d_{x^2-y^2}$
QW2'	Minority	$A$	$d_{xy}$
QW2	Majority	$A$	$d_{x^2-y^2}$
QW2'	Majority	$A$	$d_{xy}$
QW3	Majority	$A$	$d_{z^2}$

representation (linear combination of the  $s$  and all the  $p$  and  $d$  atomic orbitals).<sup>30</sup> Our numerical results are in agreement with this orbital description. Tables II and III summarize the symmetry of the electron states when  $\mathbf{k}_{\parallel}$  is along  $\bar{\Gamma}\bar{M}$  and  $\bar{\Gamma}\bar{K}$ . Most of the time, one or several terms dominate in the linear combination of atomic orbitals which describes the electron states: These main contributions are indicated in the tables. Note that states with the  $E$  symmetry at  $\bar{\Gamma}$  usually split in states with  $A'$  and  $A''$  symmetry, while states with the  $A_1$  symmetry at  $\bar{\Gamma}$  belong to the  $A'$  symmetry for  $\mathbf{k}_{\parallel}$  along  $\bar{\Gamma}\bar{M}$ .

The conclusions which have been obtained for Co(1ML)/Ni(111) can be generalized for thicker Co overlayers. The dispersion curves are however much more complicated because of the high number of QW states which exist in this case.

#### IV. TOTAL DENSITY OF STATES AND SPIN POLARIZATION AT THE OVERLAYER SURFACE

We have calculated the total DOS for all the overlayers. Results for energies below the Fermi level can be used to analyze the photoemission spectra recorded at the Co( $n$ MLs)/Ni(111)

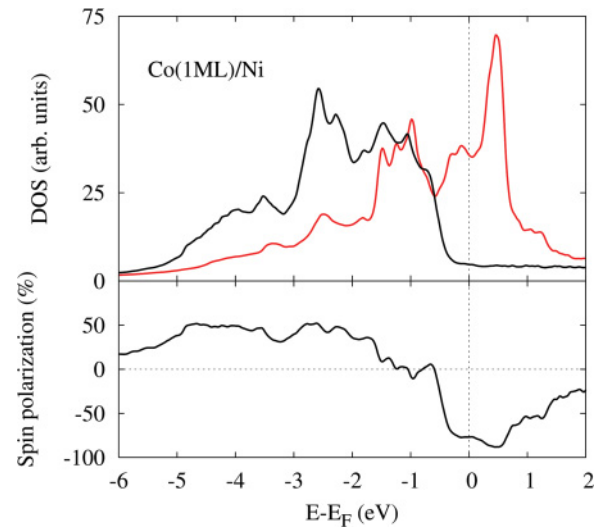


FIG. 5. (Color online) Majority spin (dark line) and minority spin (red line) total DOS for a surface Co atom of the Co(1ML)/Ni(111) overlayer (top part of the figure) and corresponding spin polarization (bottom part of the figure).

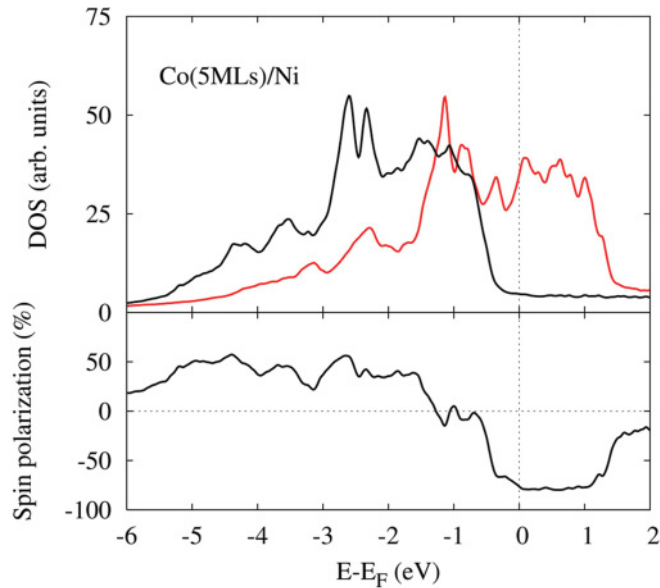


FIG. 6. (Color online) Same as in Fig. 5, but for the Co(5MLs)/Ni(111) overlayer.

surfaces. Some of the results are displayed in Figs. 5 and 6. The majority spin  $d$  bands are fully occupied for all the overlayers and the main differences between the DOS of the different systems can be observed on the minority spin  $d$  states which cross the Fermi level. When the overlayer consists of a single Co atomic plane, the density of unoccupied minority spin states integrated over a Co surface atom possesses a strong peak near 0.47 eV while the DOS shows a more broadened structure for occupied states between  $-1.6$  and  $-0.8$  eV; see Fig. 5. The majority spin DOS is not strongly different for a surface Co atom of the Co(5MLs)/Ni overlayer, as shown in Fig. 6. The minority spin DOS differs in this case, in particular just before the Fermi level where the DOS curve passes by a minimum, and above  $E_F$  where the DOS is more broadened than for Co(1ML)/Ni.

The spin polarizations for a Co atom of the Co(1ML)/Ni and Co(5MLs)/Ni overlayers only differ above the Fermi level. This means that the differences between the spin polarizations measured in photoemission experiments for different Co/Ni overlayers will not originate from the topmost atomic layer but from the second (and to a less extent from the third) monolayers which will be formed by Ni atoms in the case of Co(1ML)/Ni and by Co atoms for thicker Co layers. For unoccupied states, the spin polarization for a surface Co atom of the Co(5MLs)/Ni is nearly identical to that of a clean (111) fcc Co surface.

The total DOS curves can also be used to calculate the spin magnetic moments of the different atoms. We found that the magnetic moment of a surface Co atom is slightly enhanced at the surface (between 2.7% and 4.5% depending of the overlayer thickness) while it is identical to the bulk fcc Co value for the interface Co atom. The spin magnetic moment of the interface Ni atom is also higher (up to 3%) at the Ni/Co interface than in bulk Ni.

## V. SUMMARY

We used the first-principles code layer-KKR to calculate the electronic structure in Co( $n$ MLs)/Ni(111) overlayers as a function of the Co thickness. Peaks in the DOS curves show that localized electron states can exist in these systems. We identified their nature, QW or surface states, by comparing the results with those calculated for analogous Ni/Co( $n$ MLs)/Ni(111) buried QWs. We found that the energy of the surface states is the same for all the overlayers thicker than 2 Co MLs, while the number of QW states increases with the Co thickness. We described the dispersion and the orbital character of these states along the  $\bar{\Gamma}M$  and  $\bar{\Gamma}K$  directions. For the surface atomic layer, the total density of occupied states poorly depends on the number of Co MLs deposited on the substrate, which means that the spin polarization differences measured for the different systems are essentially due to the nature (Co or Ni) of the subsurface layer. These results could help to interpret surface-sensitive spectra recorded *in situ* during the growth of Co/Ni(111) multilayers.

<sup>1</sup>B. Feuerbacher and B. Fitton, *Phys. Rev. Lett.* **29**, 786 (1972).

<sup>2</sup>N. D. Lang, *Phys. Rev. B* **34**, 5947 (1986).

<sup>3</sup>S. Mangin, D. Ravelosona, J. A. Katine, M. J. Carey, B. D. Terris, and E. F. Fullerton, *Nature Mater.* **5**, 210 (2006).

<sup>4</sup>S. Girod, M. Gottwald, S. Andrieu, S. Mangin, J. McCord, E. E. Fullerton, J. M. L. Beaujour, B. J. Krishnatreya, and A. D. Kent, *Appl. Phys. Lett.* **94**, 262504 (2009).

<sup>5</sup>F. J. Himpsel and D. E. Eastman, *Phys. Rev. Lett.* **41**, 507 (1978).

<sup>6</sup>G. Borstel, G. Thörner, M. Donath, V. Dose, and A. Goldmann, *Solid State Commun.* **55**, 469 (1985).

<sup>7</sup>J. Kutzner, R. Paucksch, C. Jabs, H. Zacharias, and J. Braun, *Phys. Rev. B* **56**, 16003 (1997).

<sup>8</sup>J. Braun and M. Donath, *Europhys. Lett.* **59**, 592 (2002).

<sup>9</sup>M. Donath, F. Passek, and V. Dose, *Phys. Rev. Lett.* **70**, 2802 (1993).

<sup>10</sup>K.-F. Braun and K.-H. Rieder, *Phys. Rev. B* **77**, 245429 (2008).

<sup>11</sup>F. Mittendorfer, A. Eichler, and J. Hafner, *Surf. Sci.* **423**, 1 (1999).

<sup>12</sup>T. Ohwaki, D. Wortmann, H. Ishida, S. Blügel, and K. Terakura, *Phys. Rev. B* **73**, 235424 (2006).

<sup>13</sup>C. L. Fu and A. J. Freeman, *J. Phys. Colloques* **49**, C8-1625 (1988).

<sup>14</sup>M. Alden, S. Mirbt, H. L. Skriver, N. M. Rosengaard, and B. Johansson, *Phys. Rev. B* **46**, 6303 (1992).

<sup>15</sup>F. J. Himpsel and D. E. Eastman, *Phys. Rev. B* **20**, 3217 (1979).

<sup>16</sup>F. J. Himpsel and D. E. Eastman, *Phys. Rev. B* **21**, 3207 (1980).

<sup>17</sup>E. Wetli, T. J. Kreuzt, H. Schmid, T. Greber, J. Osterwalder, and M. Hochstrasser, *Surf. Sci.* **402–404**, 551 (1998).

<sup>18</sup>C. Math, J. Braun, and M. Donath, *Surf. Sci.* **482–485**, 556 (2001).

<sup>19</sup>S. N. Okuno, T. Kishi, and K. Tanaka, *Phys. Rev. Lett.* **88**, 066803 (2002).

<sup>20</sup>M. A. Barral, M. Weissman, and A. M. Llois, *Phys. Rev. B* **72**, 125433 (2005).

<sup>21</sup>O. Hjortstam, J. Trygg, J. M. Wills, B. Johansson, and O. Eriksson, *Phys. Rev. B* **53**, 9204 (1996).

- <sup>22</sup>K. Kyuno, J.-G. Ha, R. Yamamoto, and S. Asano, *Jpn. J. Appl. Phys.* **35**, 2774 (1996).
- <sup>23</sup>C. Hwang and F. J. Himpsel, *Phys. Rev. B* **52**, 15368 (1995).
- <sup>24</sup>S. S. Dhesi, H. A. Dürr, G. van der Laan, E. Dudzik, and N. B. Brookes, *Phys. Rev. B* **60**, 12852 (1999).
- <sup>25</sup>S. S. Dhesi, H. A. Dürr, E. Dudzik, G. van der Laan, and N. B. Brookes, *Phys. Rev. B* **61**, 6866 (2000).
- <sup>26</sup>A. Ernst, G. van der Laan, W. M. Temmerman, S. S. Dhesi, and Z. Szotek, *Phys. Rev. B* **62**, 9543 (2000).
- <sup>27</sup>J. M. MacLaren, S. Crampin, and D. D. Vvedensky, *Phys. Rev. B* **40**, 12176 (1989).
- <sup>28</sup>J. M. MacLaren, S. Crampin, D. D. Vvedensky, R. C. Albers, and J. B. Pendry, *Comput. Phys. Commun.* **60**, 365 (1990).
- <sup>29</sup>B. P. Tonner, Z.-L. Han, and J. Zhang, *Phys. Rev. B* **47**, 9723 (1993).
- <sup>30</sup>M. S. Dresselhaus, G. Dresselhaus, and A. Jorio, *Group Theory, Applications to the Physics of Condensed Matter* (Springer Verlag, 2008).
- <sup>31</sup>R. H. Victora and L. M. Falicov, *Phys. Rev. B* **28**, 5232 (1983).
- <sup>32</sup>R. Mazzarello, A. Dal Corso, and E. Tosatti, *Surf. Sci.* **602**, 893 (2007).
- <sup>33</sup>C. S. Wang and J. Callaway, *Phys. Rev. B* **15**, 298 (1977).
- <sup>34</sup>J. R. Anderson, D. A. Papaconstantopoulos, L. L. Boyer, and J. E. Schirber, *Phys. Rev. B* **20**, 3172 (1979).
- <sup>35</sup>F. Gibmert and L. Calmels, *J. Appl. Phys.* **109**, 07C109 (2011).